High-Strain Deformation of Polyethylenes in Plane-Strain Compression at Elevated Temperatures

E. Lezak, Z. Bartczak

Centre of Molecular Macromolecular Studies, Polish Academy of Sciences, Sienkiewicza 112, 90-363 Lodz, Poland

Received 24 February 2006; accepted 28 March 2006
DOI 10.1002/app.26011
Published online in Wiley InterScience (www.interscience.wiley.com).

ABSTRACT: The deformation and recovery behavior of several polyethylenes and ethylene-based copolymers with various molecular architectures and a broad range of molecular masses and molecular mass distributions was studied. Because of the differences in the molecular characteristic, this series exhibited a relatively broad range of crystallite sizes and crystallinity levels. The samples were subjected to high strain compression under plane-strain conditions at the elevated temperature of 80°C. The unloading of the compressed samples led to substantial nonelastic recovery of the strain. The stress–strain and recovery behavior was related to the molecular parameters. The results confirmed the common deformation scheme with four crossover points related to the activation of subsequent deformation mechanisms, as proposed by Strobl. Although the critical strains, related to the activation of deformation of the crystalline component, are invariant, the critical strain of the last point, which is related to the activation of chain disentanglement in the amorphous component, depends on the temperature of deformation. That critical strain decreases from 1.0 to approximately 0.8–0.9 as the temperature of deformation increases from room temperature to 80°C. This shift results from an increase in the chain mobility with increasing temperature, and this makes modification of the molecular network through chain disentanglements easier. © 2007 Wiley Periodicals, Inc. J Appl Polym Sci 105: 14–24, 2007

Key words: compression; polyethylene (PE); strain

INTRODUCTION

In two recent articles,[1,2] we reported studies of the deformation in plane-strain compression[1] and postloading recovery behavior[2] of series of various polyethylenes and ethylene-based copolymers covering a broad range of chain architecture, molecular weights, and crystalline structures. The results allowed us to extend the validity of the deformation scheme proposed recently by Strobl and coworkers[3–8] for tension toward deformation in compression. The crucial role of the molecular network within the amorphous phase and the influence of its properties on the deformation behavior were also demonstrated.[1,2]

The main characteristic of the deformation scheme proposed by Strobl et al.[3] is that the deformation is controlled by the strain rather than the stress. Along the true-stress/true-strain curves, four characteristic points have been identified and ascribed to the activation of subsequent deformation mechanisms: (A) isolated and (B) collective crystallographic slip, giving rise to the yield point, (C) crystal fragmentation/fibrillation, and (D) disentanglement of chains in the amorphous component. The critical strains at which these points are located are practically invariant with respect to the strain rate and drawing temperature,[4,7] as well as the crystallinity of a polymer.[1–3,5,7] In contrast, the corresponding stresses vary significantly with the crystallinity and with the strain rate or temperature.[3,4,7] From a global point of view, the deformation of a semicrystalline polymer may be considered the stretching of a macromolecular network in which entanglements and crystallites act as physical junctions. Crystallites experience textural transformations according to crystallographic mechanisms in parallel with the network stretching. However, these transformations do not impede the deformation processes in amorphous layers. Upon deformation, the load is transmitted by crystallites and the molecular network of the amorphous regions, yet the respective weights change with the advance of the deformation process.[3] The network forces, initially low, become dominant over those associated with the plastic deformation of crystals at high strain. The crossover point seems to be point C of the deformation scheme, around the true strain of 0.6–0.7,[3] at which the stresses generated in the stretched network of amorphous chains become high enough to trigger fragmentation of adjacent crystallites.[2,3]

The deformation of crystals through various crystallographic mechanisms is permanent, whereas that

This article is dedicated to the memory of Professor Marian Kryszewski

Correspondence to: Z. Bartczak (bartczak@bilbo.cbmm.lodz.pl).

Contract grant sponsor: State Agency for Scientific Research of Poland; contract grant number: 7 T08E 036 19.
Contract grant sponsor: Budget Sources for Science (2005–2008); contract grant number: 3T08E 007 28.

of the rubbery amorphous component appears at least partially reversible. To produce a really irreversible deformation of polyethylene, it is necessary to deform it to a strain above 1.0[2,3] (point D of Strobl et al.'s scheme).[3] At this strain, chains in the amorphous network start to disentangle. This leads to the permanent, irreversible deformation of the amorphous component in addition to irreversible plastic deformation of the crystalline component, and consequently, the memory of the undeformed macrostate of the material is lost.

Strobl and coworkers[4,7] postulated an invariance of the critical strains of the proposed deformation scheme with respect to the deformation rate and temperature. Taking that into account, we decided to limit our first experiments[1,2] to a single temperature (room temperature) and deformation rate. In what follows, we describe the results of a supplementary study of deformation at an elevated temperature. The temperature of 80°C was chosen as the deformation temperature. At this temperature, the α-relaxation process of polyethylene is already well advanced, whereas the melting point is still far enough away. Similarly to the previous study,[1,2] the deformation was produced by plane-strain compression; this mode is advantageous over other modes because the deformation is homogeneous with no instabilities, such as necking, frequently observed in tension. Moreover, the cavitation is inhibited in this deformation mode because of external constraints.[1]

The same set of polyethylene samples used in refs. 1 and 2, demonstrating similar morphologies yet very different molecular characteristics and different levels of overall crystallinity, was used in this investigation.

EXPERIMENTAL

Materials and sample preparation

The materials used in this study were samples of several grades of commercial polyethylenes, including linear high-density polyethylenes (HDPEs; code H) of various molecular weights, ultrahigh-molecular-weight polyethylenes (UHMWPEs; code U), conventional branched low-density polyethylenes (code L) of different branching levels and molecular weights, linear low-density polyethylenes (code LL), and ethylene-based copolymers (i.e., ethylene–octene elastomers; code E). These materials were the same as those investigated in refs.1 and 2. Their characteristics are presented in Table I.

The samples, in the form of 50 × 50 × 4 mm^3 plates, were prepared by compression molding at 190°C (230°C for UHMWPE) and 50 atm. The compressed plates were solidified by rapid cooling in an iced water. Specimens of a size appropriate for particulate deformation experiments were machined from the cores of these plates. All samples were prepared according to the same thermal protocol to obtain similar supermolecular structures in all materials. All, except UHMWPEs U-1 and U-2, exhibited similar spherulitic morphologies.[1] Their crystallinities and long periods are listed in Table I.

Deformation and recovery experiments

Plane-strain-compression tests were performed with the loading frame of an Instron model 5582 universal tensile testing machine (Canton, MA) and a compression tool of the channel-die type, which was

TABLE I
Characteristics of the Polymers

Sample	Manufacturer	M_w (g/mol)	M_w/M_n	Number of branches (1/1000C)	Melt flow index (g/10 min)[a]	Crystallinity (wt %)[b]	Long period (nm)[c]
H-1	Quantum (Cincinnati, OH)	0.57×10^5	3.5	<0.1	6.7	72.7	23.5
H-2	BASF (Ludwigshafen, Germany)	0.76×10^5	4.4	<0.1	7	73.3	23.3
H-3	BASF	1.20×10^5	3.4	<5	2.3	62.6	22.2
H-4	BASF	1.83×10^5	7.2	<0.2	0.2	67.7	24.4
H-5	BASF	4.78×10^5	12.2	<3	—	60.9	26.0
U-1	Ticona (Kelsterbach, Germany)	$\sim 2 \times 10^6$			—	48.9	33.3
U-2	Ticona	$\sim 5.5 \times 10^6$			—	49.6	33.3
L-1	BASF	2.5×10^5		20	3.4	46.3	13.2
L-2	BASF	3.3×10^5		24	2.1	44.4	12.8
L-3	BASF	4.5×10^5	13.0	35	0.3	40.4	12.3
L-4	BASF	2.0×10^5	4.0	35	1.6	40.0	11.6
L-5	BASF	0.48×10^5	3.7	35	20	40.0	11.0
LL-1	Elenac (Ludwigshafen, Germany)	0.71×10^5	2.4	20[d]	2.5	43.0	13.9
LL-2	Elenac	0.92×10^5	4.0	20[d]	2.8	41.6	16.1
E-1	Exxon (Irving, TX)	0.82×10^5	3.7	33[d]	3	30.1	11.0

[a] At 2.16 kg and 190°C.
[b] Estimated on the basis of the heat of melting (DSC; see ref. 1).
[c] Estimated from small-angle scattering (see ref. 1).
[d] Number of short branches calculated from the molar content of the comonomer (^{13}C-NMR).

equipped with load and strain gauges as well as heaters connected to the temperature controller. Two compression tools of different sizes and geometries, shown schematically in Figure 1, were used. The dimensions of the specimens used in deep channel-die compression [Fig. 1(a)] were 3.85 × 50 × 40 mm^3 [along the constraint direction (CD), flow direction (FD), and load direction (LD), respectively], whereas those of the specimens compressed in a small die [Fig. 1(b)] were 15 × 6 × 4 mm^3 (CD × FD × LD). Other details are given in ref. 1.

All deformation experiments were performed with a constant speed of the crosshead of the loading frame. For both specimen sizes, the speed of the crosshead was set to give an initial deformation rate of 5%/min (8.3 × 10^{-4} s^{-1}). The temperature of deformation was kept at 80 ± 1°C. Each deformed specimen after reaching the desired strain was immediately unloaded and taken out from the die to allow its unconstrained recovery under the ambient conditions.

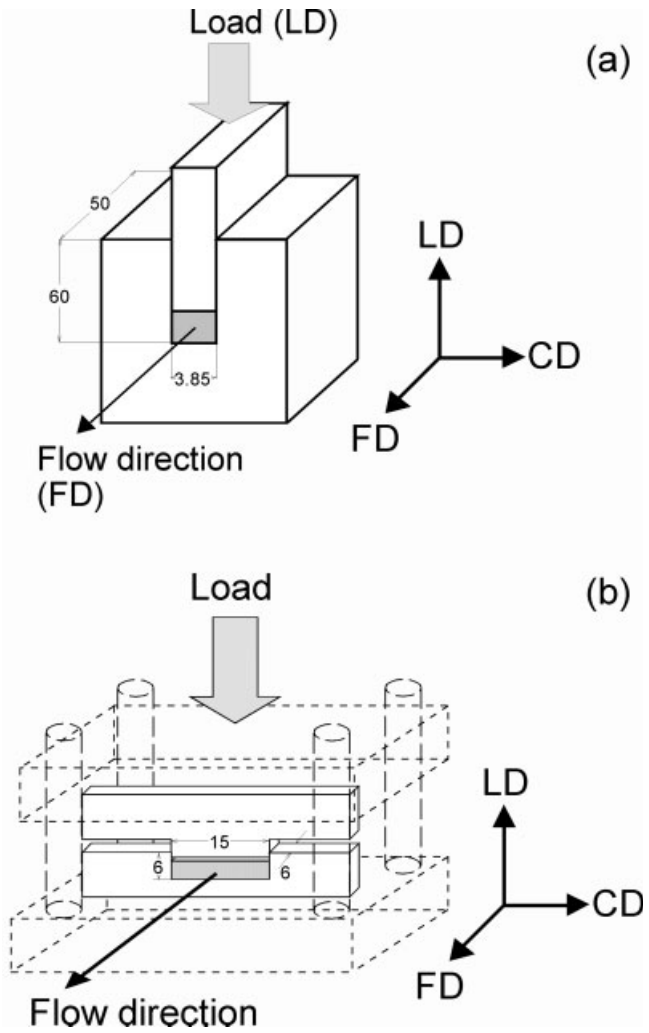

Figure 1 Deformation tools used for plane-strain compression: (a) a deep channel die and (b) a small die. The compressed sample is gray. In part b, the guidance system is shown by a broken line.

The postdeformation behavior was monitored by measurements of the dimensions of the recovering specimens. Their dimensions along FD, CD, and LD were measured repeatedly with a digital micrometer over a period of 6 weeks after unloading. The recovered and remaining strain components were calculated from the measured changes of the specimen dimensions.

In a separate experiment, the specimens, already recovered at room temperature over a long period of time (at least 6 weeks), were slowly heated in an oil bath to the temperature selected from the range between room temperature and a temperature slightly below the melting point of the particular polymer studied. Oil immersion was used to reduce any external constraint during recovery. After 10 min of annealing at a given temperature, the specimens were cooled, their dimensions were measured, and then the recovered and remaining strain components were calculated.

Thermal properties

Thermal analysis of the samples was conducted with a TA 2920 differential scanning calorimetry (DSC) apparatus (thermal analysis) (Wilmington, DE). The melting thermograms were recorded at a heating rate of 10°/min under a nitrogen flow. The crystallinity was estimated on the basis of the heat of melting of the sample; the heat of melting of 100% crystalline polyethylene was assumed to be 293 J/g.[9]

RESULTS AND DISCUSSION

Figure 2 presents the true-stress/true-strain curves determined from the load–displacement data collected during plane-strain compression at 80°C in a small die [Fig. 1(b)]. In the plane-strain-compression test, the geometry employed here, the area of the sample under load is constant and remains equal to the cross-section area of the plunger. Therefore, the true stress can be calculated readily from the load data. Because the deformation is macroscopically homogeneous in the entire range of displacement, the true strain can be calculated with the following equation:

$$e = \int_{h=h_o}^{h=0} \frac{dh}{h} = \ln\left(\frac{h_0}{h}\right) = \ln\left(\frac{h_0}{h_o - \triangle h}\right) \qquad (1)$$

where e is the true strain, h_0 denotes the initial height of the specimen, $h = h_0 - \Delta h$ represents its

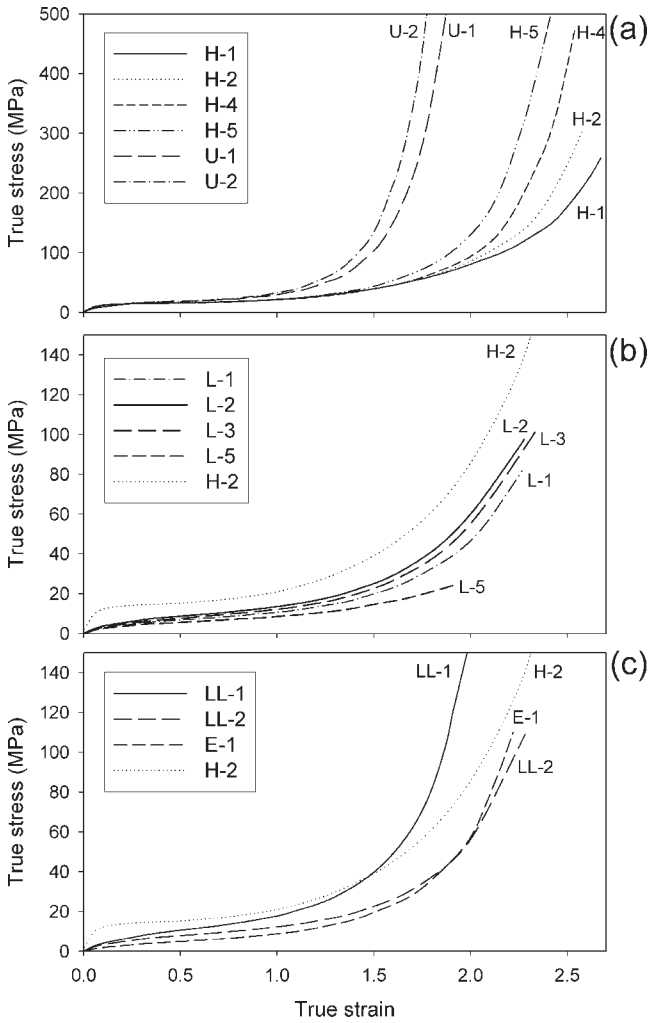

Figure 2 Representative true-stress/true-strain plots of samples deformed by plane-strain compression at 80°C: (a) linear polyethylenes, (b) branched polyethylenes, and (c) ethylene-based copolymers. In parts b and c, the curve of linear HDPE sample H-2 was added as a reference (dotted line).

actual height, and Δh is the measured displacement of the plunger. $\lambda = h_0/h$ is the compression ratio.

Figure 2(a) shows the true-stress/true-strain curves determined for samples of linear polyethylene. These curves demonstrate the same features as the curves obtained from the compression of the respective polymers at room temperature, as discussed in a previous article.[1] We note again the dependence of the yield point on the properties of the crystalline phase. The stress at yield increases with increasing crystallinity and thickness of the crystallites, as it does at room temperature. At the same time, the yield strain seems to remain invariant (point B of Strobl et al.'s deformation scheme[3]). Soon after the yielding, strain hardening sets in, initially being relatively low and becoming very intense at strains above 1.0–1.5. That strain hardening depends on the molecular weight of the polymer: its onset shifts apparently to a lower strain whereas the rate increases with increasing molecular weight. This dependence on the molecular weight is clear because the weight-average molecular weight (M_w) increases by 2 orders of magnitude within the discussed series, whereas other parameters, including the amount and properties of the crystalline phase, change to a much lesser extent at the same time; for example, the crystallinity of H-5 is only a few percent lower than that of H-1. Although the yield stresses determined at 80°C are noticeably lower than those observed in the respective samples at room temperature, the stresses generated during the strain-hardening stage are equally high at both temperatures, especially in samples of high molecular weights. The strain hardening is controlled by the response of the molecular network of entangled chains to increasing strain.[1,3,11–13] The observed dependence of on the molecular weight reflects the properties of the molecular network, which change substantially with increasing molecular weight[1] and are less sensitive to the deformation temperature.

The range of intense strain hardening moves toward higher strains with an increase in the temperature of deformation. This tendency is much more pronounced in samples of low molecular weight, in which the rate of the hardening is also substantially reduced at 80°C in comparison with room temperature.[1] This indicates that the compliance of the network of relatively short chains increases faster with increasing temperature than that of a network formed by long chains. This can suggest that a molecular network made up of short chains can relax through slippage of chains out of entanglements notably more easily than a network of long chains, especially at high temperatures of deformation. This hypothesis is confirmed later by model calculations and the results obtained from strain-recovery experiments.

Similar observations can be made for the stress–strain behavior of branched polyethylenes and ethylene-based copolymers, as illustrated in Figure 2(b,c), respectively. However, in contrast to linear polyethylenes, which usually did not break even at very high strains approaching 3, the samples of branched polyethylene fractured in the range of true strains slightly above 2 and at related stresses well below 200 MPa. Interestingly, the fracture of branched samples occurred at strains only a little higher than those observed upon the fracture of the respective material at room temperature. Apparently, the ultimate properties of a more constrained network of branched chains do not change with temperature as much as the properties of networks of linear chains.

To find the deformation-induced changes in the crystalline component, the crystallinity of samples

TABLE II
Temperature of the Melting Peak and Crystallinity Determined from DSC Heating Scans at a Heating Rate of 10°C/min

	Annealed at 80°C		Deformed at 80°C			
Sample	Melting temperature (°C)	Crystallinity (wt %)	Applied strain	Permanent strain	Melting temperature (°C)	Crystallinity (wt %)
H-1	132.1	74.8	2.00	1.88	133.1	74.2
H-2	132.7	78.1	2.00	1.98	133.7	75.0
H-4	133.7	72.1	2.00	1.78	134.5	68.9
H-5	132.7	67.8	2.00	1.80	134.2	61.5
U-1	131.1	49.0	1.75	1.39	132.3	44.8
U-2	131.7	48.4	1.68	1.35	132.3	44.6
L-2	111.7	44.1	1.75	111.5	41.8	61.5
L-3	108.2	41.0	1.98	1.70	108.3	38.8
LL-1	113.3	40.4	2.00	1.65	117.1	37.6
LL-2	121.8	40.5	2.00	1.64	122.3	36.7
E-1	94.6	31.7	2.00	1.39	96.5	34.8

deformed to a true strain around 2 was determined by DSC. For reference, specimens of unoriented material of the same thermal history, that is, specimens annealed at the deformation temperature of 80°C for a time similar to the duration of the compression experiment, were also investigated. Table II presents the results. These data demonstrate a small increase in the melting temperature in all deformed samples, whereas their crystallinities slightly decrease in comparison with those of the undeformed counterparts. The increase in the melting temperature reflects an increasing average length of the crystalline stem, which thus increases the average thickness of the lamellae. Such changes in the crystalline component result from fragmentation and partial destruction of the lamellar structure, occurring at a strain near 0.6 and above.[1–4,13] The partial destruction of lamellae leads to a reduction of the overall crystallinity. On the other hand, lamellae break preferentially at points of the smallest thickness; therefore, the average thickness and hence the melting temperature will increase.[13] Because of the local character of these phenomena, their influence on the melting temperature and crystallinity is limited.

The strain-hardening behavior of a semicrystalline polymer manifesting above the yield point can be ascribed to the entropy–elastic response of the molecular network of entangled chains upon its deformation.[3,10,11] Model calculations have demonstrated that the stress associated with the deformation and orientation of the crystalline component remains nearly constant over a wide range of strains or rises slowly with increasing strain, depending on the mode of deformation, whereas the stress associated with the orientation of the molecular network of the amorphous phase increases substantially at the same time.[12] This allows us to conclude that just the deformation of the molecular network is the main source of the stress-hardening behavior. The observations of strain hardening, reported previously, support this conclusion.

To characterize the strain-hardening behavior of the network, the moduli of the initial strain hardening were estimated from the stress–strain curves. This was accomplished by the fitting of the experimental curves to curves calculated with a simple one-dimensional model involving a rubber–elastic response of the molecular network within the amorphous component and based on the hypothesis of Haward and Thackray.[10] According to this hypothesis, the strain hardening of the material, originating from stretching of the molecular network of entangled chains, can be represented in the model by the nonlinear spring element, which is connected in parallel to a viscoplastic dashpot representing the rate- and temperature-dependent yield and viscoplastic flow.

Because the response of the molecular network was in focus here, several simplifying assumptions were made in the model formulation: the material was assumed to be incompressible, and its initial elastic deformation was neglected as the respective strain was small in comparison with the total strain. Next, the viscoplastic response was reduced to a purely plastic one, represented by the plastic flow stress alone. The strongest simplification was that any relaxation phenomena within the network were not taken into account, whereas in the real system, such processes can play quite important roles and lead to the accommodation of a part of the imposed strain, especially at elevated temperatures. Because of these serious simplifications, only raw, semiquantitative estimations were expected.

Under these assumptions, the true stress generated in the system can be simply represented as follows:[11,14]

$$\sigma = Y + \sigma_R \tag{2}$$

where σ is the true stress, Y is the plastic flow stress, and σ_R is the rubberlike true stress generated by entangled molecular networks. σ_R was modeled with non-Gaussian chain statistics and the eight-chain model developed by Arruda and Boyce.[15] For the plane-strain compression, the equation for the stress in the LD takes the following form:

$$\sigma_R = \frac{G_n}{3}\sqrt{n}\frac{1}{\lambda_{\text{chain}}}L^1\left(\frac{\lambda_{\text{chain}}}{\sqrt{n}}\right)\cdot\left(\lambda^2-\frac{1}{\lambda^2}\right) \qquad (3)$$

where $G_n = N_e kT$ is the initial strain-hardening modulus of the network (N_e is the effective crosslink density, k is the Boltzmann constant, and T is the temperature); n is the number of rigid links between effective crosslinks (entanglements and junctions at amorphous–crystal interfaces provided by tie molecules), setting the extensibility limit of a chain in the network ($\lambda_{\max} = n^{1/2}$); and λ_{chain} is the stretch on each chain in that network, given by the root mean square of the applied strain: $\lambda_{\text{chain}} = [1/3(\lambda^2 + 1 + 1/\lambda^2)]^{1/2}$. $L^{-1}(x)$ denotes the inverse Langevin function [$L(x) = \coth x - 1/x$, where $x = \lambda_{\text{chain}}/n^{1/2}$]. For large values of n, there is no limiting extensibility of the network, and eq. (3) can be reduced to the well-known Gaussian equation (plane-strain deformation):

$$\sigma_R = G_n\left(\lambda^2-\frac{1}{\lambda^2}\right) \qquad (4)$$

The experimental true-stress/true-strain curves were fitted in the strain range of 0.1–2.5 with eqs. (2) and (3). The fit parameters were Y, G_n, and n. The fits employing Gaussian chain statistics [eq. (2) combined with eq. (4)] were also performed. Figure 3 presents representative true-stress/λ curves calculated for linear and branched polyethylene samples (both Langevin and Gaussian fits are shown) and the respective experimental curves. A general observation is that the experimental stress–strain curves can be approximated successfully with Gaussian curves [eq. (4)] in the range of the initial strain hardening, up to relatively high λ values of 3–4.5 (true strain = 1.0–1.5), before the onset of the final intense strain hardening. At higher strains, the stress predicted by the Gaussian fit was, however significantly lower than that observed experimentally. Thus, the application of the non-Gaussian chain statistics [eq. (3)] was necessary to get better agreement in the high strain range, although even then the fit was not satisfactory: the calculations usually predicted too fast a rise of the stress in the final part of the curve. On the other hand, for samples of relatively low molecular weights, such as linear polyethylenes H-1 and H-2 and branched L-5 ($M_w = 0.5$–0.7×10^5), the experimental curves could be fitted quite well even with a simple Gaussian equation in nearly the full range of the strain.

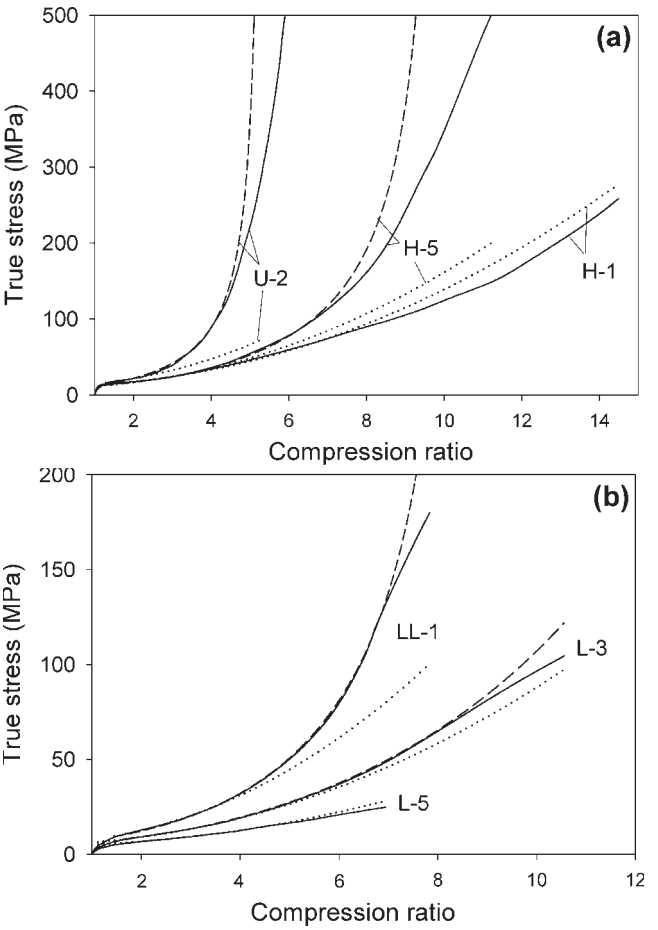

Figure 3 Representative fits obtained for samples of (a) linear and (b) branched polyethylenes. The solid line is the experimental true-stress/true-strain curve, the dashed line is the curve fit with the Langevin equation [eq. (3)], and the dotted line is the curve fit with the neo-Hookean equation [eq. (4)].

It appears that neither model is accurate enough to capture precisely the entire strain range, probably because of the simplified formulations. Nevertheless, the agreement of the calculated curves with the experimental ones at $\lambda < 3$–4 (Gaussian fits) or $\lambda < 7$ (non-Gaussian fits) is very good, and this suggests that the values of the hardening modulus of the network determined in this strain range can be considered reasonable.

Table III summarizes the best fit values of G_n and n. They are compared with the respective values obtained at room temperature and taken from ref. 1. G_n, estimated at 80°C, varies in a manner similar to that observed previously at room temperature,[1] although the values of G_n obtained at 80°C are roughly only half of those determined at room temperature. A general trend, observed at both temperatures, is an increase in the network modulus with increasing molecular weight. This dependence on

TABLE III
Comparison of G_n and n Values Estimated from Deformation Experiments at Room Temperature (22°C) and 80°C

	22°C[a]		80°C[b]	
Sample	G_n	n	G_n	n
H-1	1.82	22	1.09	∞
H-2	1.91	21	1.14	∞
H-4	1.99	19	1.15	80
H-5	2.25	14	1.17	35
U-1	3.90	13	1.99	12
U-2	5.11	13	2.29	10
L-1	1.47	23	0.61	130
L-2	1.60	23	0.71	130
L-3	1.82	22	0.76	130
L-4	1.60	22	0.80	110
L-5	1.37	31	0.42	∞
LL-1	1.99	23	1.17	28
LL-2	1.65	26	0.66	65
E-1	1.56	25	0.65	53

[a] See ref. 1.
[b] This work.

the molecular weight is discussed in ref. 1. It has been demonstrated that the density of entanglements constituting the network in the amorphous component, controlling the strain hardening, is larger than that in the melt before sample crystallization because the entanglements present in the melt are usually not resolved during the growth of crystallites but are only rejected into and concentrated in amorphous layers between them. Actually, in polymers of relatively low molecular weights, a certain fraction of entanglements of chains attaching to the crystal can be resolved by diffusion through a relatively short reptation tube. The time set by crystallization kinetics can be sufficiently long to allow that. The resulting molecular network in the amorphous component demonstrates then a density of entanglements not much higher than that in the melt.[1] However, the time necessary for diffusion through the reptation tube (τ_r) increases considerably with increasing chain length M ($\tau_r \propto M^3$) and soon becomes longer than the accessible time, set by the kinetics of crystallization, which is generally independent of M. This, in turn, leads to an increase in the number of entanglements to be redistributed into amorphous layers of limited volume when the molecular weight increases. Consequently, the local density of entanglements in the amorphous component increases with increasing molecular weight. The density of the molecular network in a sample of solidified polyethylene of high molecular mass is considerably higher than in a sample of low molecular mass crystallized under similar conditions or in the melt. This trend is clearly demonstrated by the series of linear polyethylenes (H-1 to H-5 and U-2) of increasing molecular weight and relatively little variation in crystallinity, exhibiting a noticeable increase in the network modulus (proportional to N_e) with increasing molecular weight.

Another parameter influencing the network density is the architecture of the chain: the presence of long or short branches (comonomer units) hinders crystallization, leading to lowered crystallinity (i.e., lesser redistribution of entanglements than in highly crystalline linear polyethylenes), and chain disentanglement by their reptation (fewer entanglements can be resolved because of steric hindrance between the chains). As a result, the network density and consequently the strain-hardening behavior depend on the type and number of branches distributed along the chain, in addition to the molecular weight dependence.

The data for the strain-hardening modulus presented in Table III demonstrate the negative temperature dependence. This finding is in conflict with the concept of an entropy–elastic network response, which predicts the strain-hardening modulus to be proportional to the absolute temperature. A similar decrease in the strain-hardening modulus with increasing temperature was, however, also observed in several amorphous[16–19] and semicrystalline[20,21] polymers. On the other hand, the hardening modulus was proportional to the network density, regardless of the nature of the network, that is, the physical entanglements or chemical crosslinks,[19] and this clearly points to the molecular network as a source of strain hardening. It has been proposed that such a negative temperature dependence of the strain hardening originates from a change (decrease) in the number of elastically active chains (i.e., N_e), which is equivalent to a change in the number of segments between entanglements (i.e., n), because the total number of units is conserved.[16] A possible reason for such a decrease is the relaxation of the stressed molecular network, which is more intense at a high temperature of deformation because the chain entanglements constituting the network are mobile at the deformation temperature, which is higher than the glass-transition temperature. Moreover, it is well known that even the mechanical response of chemically crosslinked rubbers can be strongly influenced by the stress relaxation and that rubber elasticity holds strictly only for the equilibrium modulus.[20] Therefore, it seems justified to relate the strain-hardening response decreasing with temperature to the viscoelastic relaxation of the entangled network: the relaxation phenomena might overrule the entropic contribution of the molecular network and lead to the negative temperature dependence of the strain-hardening modulus. Because such a network relaxation process depends on the molecular weight,[20] it can be anticipated that the variation of the strain hardening with the temperature should be influenced by the molecular weight.

The other possible reason for a decrease in the network density with the temperature could be that the deformation temperature of 80°C is above the α-relaxation process of polyethylene, in which crystals are known to yield readily, and the influence of crystallites acting as physical crosslinks (i.e., the contribution of tie molecules to the network) can be considered greatly reduced or even absent.[21,22] This in turn should bring down notably the effective number of active crosslinks in the molecular network and consequently reduce the strain-hardening modulus.

None of these phenomena were taken into account in the model formulation. However, the evolution of length parameter n with the molecular weight and temperature (cf. Table III) strongly supports the hypothesis of network relaxation. The network in low-molecular-weight polyethylene (H-1, H-2, and L-5) shows an extensibility limit at room temperature ($\lambda_{max} = n^{1/2} = 4.5$) and practically does not at 80°C (the stress–strain curves can be fitted with the Gaussian model). In the case of H-1 the experimental stress–strain curve at high strains even departs slightly down from the curve predicted by the Gaussian model. The only source of such behavior is the strong relaxation of the network through the slippage of chains out of entanglements at elevated temperatures. On the contrary, the high-molecular-weight samples (U-1 and U-2), expected to exhibit considerably weaker relaxation, demonstrate similar limits of the extensibility of chains in the network at both room temperature and 80°C ($n = 10$–13).

Additional information about the network properties can be obtained from the postdeformation strain-recovery tests. Specimens 40 mm high were deformed in a deep channel die [Fig. 1(a)] to the selected strains within the range of true strains of 0–2. Large specimens were used in this experiment for better accuracy of the size measurements. After the unloading, the dimensions of the unconstrained specimen (out of the die) were monitored at room temperature over a period of time. After 6 weeks, when no further changes in the dimension were detected, the specimens were heated and annealed at increasing temperatures between room temperature and the melting temperature of a given polymer. The specimen dimensions were then examined after each annealing step. The respective strain components were calculated from the measured changes in the specimen dimensions. No studied sample changed in its width, that is, in the dimension along CD in the channel die, which practically always remained equal to the initial specimen width. That invariance confirms the plane-strain conditions of deformation (strain component $e_3 = 0$). The height of the specimens (along LD) increased during recovery with the time and/or temperature, whereas their length (along FD) decreased at the same moment. The variation of strain component e_2 along FD followed approximately inversely that of strain component e_1 along LD. Therefore, in the following, we discuss only e_1.

The applied strain ($e = e_1$) can be decomposed into two components: the recovered part (e_r) and the remaining part (e_p; i.e., the permanent part in the timescale of the experiment):

$$e = e_r + e_p \tag{5}$$

Knowing the strain left after recovery at a given time/temperature, we can calculate the recovered strain component from this equation. Figure 4 illustrates the evolution of the recovered strain component with the time and temperature for selected polymers, all deformed to the same true strain of 2. In all plots of the recovered strain versus time [Fig. 4(a)], the experimental points plotted at 0.01 h represent the first measurement taken immediately after sample unloading and its withdrawal from a channel die while the sample was still hot. The sample reached room temperature within a 20-min period before the next measurement.

The recovered component of the strain consists of an instantaneous elastic strain and a time-dependent quasielastic part. This second time-dependent part can be ascribed to the partial reversibility of the deformation of the rubbery, amorphous component because the crystalline component, after the initial elastic stage, deforms further plastically through crystallographic slips and other supplementary mechanisms of a crystallographic nature.[13,23] This plastic process is irreversible. On the contrary, the deformation of the amorphous phase through the shear of thin, amorphous, rubberlike layers between lamellae appears partially reversible.[1–3]

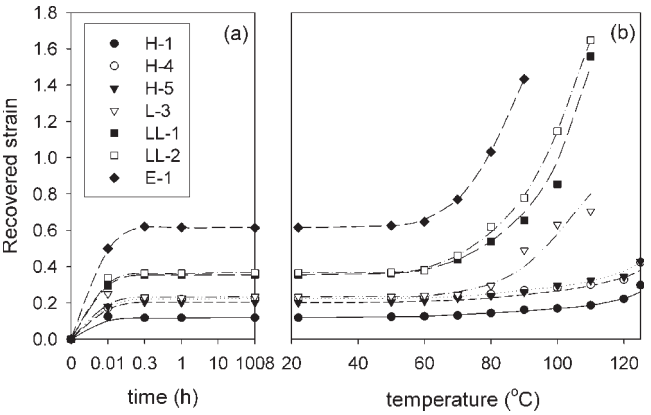

Figure 4 Evolution of the recovered component of the strain with (a) the time and (b) the temperature for samples of the indicated polymers deformed in a deep channel die to the true strain of 2.0 at 80°C.

An examination of the time dependence of the strain recovery at room temperature [Fig. 4(a)] demonstrates that most of the recovery occurred almost immediately after unloading, when the specimen was cooled from 80°C to room temperature, and the recovery was complete within the first hour after the deformation experiment for all polymers studied. This behavior is slightly different from that observed in respective materials after compression at room temperature.[2] The strain recovery at room temperature extended frequently over 1 month after specimen unloading, especially in high-molecular-weight samples. It seems that here the recovery process is arrested by the decrease in the temperature of the material from the deformation temperature of 80°C to room temperature. Apparently, the respective relaxation times increase so much with decreasing temperature that the strain remaining in the material appears stable in the timescale of the experiment (several weeks). As demonstrated by results obtained at higher temperatures [Fig. 4(b)], the recovery remained frozen up to approximately 50–60°C, that is, below the activation of the α-relaxation process, and was reactivated at temperatures approaching the temperature of deformation. At the deformation temperature and above it, the recovered strain rose substantially.

Figure 5 shows the dependence of the recovered strain component after a 6-week recovery period at room temperature on the strain applied in the plane-strain compression at 80°C. The curves are very similar to those obtained previously for the same polymers deformed at room temperature and reported in ref. 2. Both sets exhibited a low and broad maximum centered near the applied strain of 0.6–0.7 followed by a plateau of lower recovery at strains above 1.0. Furthermore, for most polymers studied, the amounts of the recovered strain after deformation at 80°C

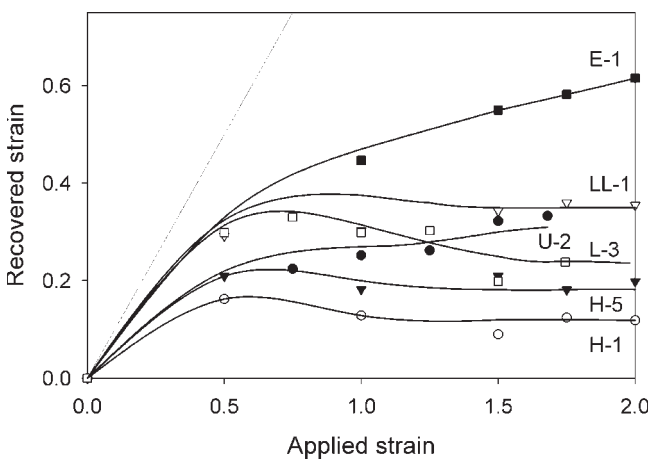

Figure 5 Recovered component of the strain of the indicated samples deformed at 80°C, determined after a 6-week recovery period at room temperature.

match quite well those observed in the respective polymers after deformation and recovery under the ambient conditions. The only departure from this scheme is the E-1 copolymer, which demonstrates higher recovery after deformation at 80°C than after deformation at room temperature and, moreover, does not show any maximum in the recovery curve after deformation at 80°C. Such behavior is probably due to partial melting of the crystalline phase of that copolymer occurring at the deformation temperature of 80°C. As revealed by DSC,[1] the peak of melting of E-1, with a maximum near 96°C, has a broad, low-temperature shoulder. Heating to the temperature of deformation causes then a noticeable increase in the amorphous fraction due to the melting of the smallest crystallites and consequently higher reversibility of deformation in comparison with deformation performed at room temperature, at which the phase composition is not altered.

The very similar recovery behavior at room temperature of samples deformed either at room temperature or at 80°C demonstrates that the change in the temperature does not have any effect on the deformation sequence. The maximum of the recovered strain curve occurs in the same true strain range of 0.6–0.7, being independent of the temperature of deformation. In addition, the plateau of the low recovered strain component develops at the same strain near 1.0. That maximum was assigned to the exhaustion and locking of interlamellar shear triggering quickly the fragmentation of lamellae (point C of Strobl et al.'s deformation scheme[3]), whereas the final plateau was interpreted as a result of a weighty erosion of the molecular network through disentanglements of chains of the amorphous component due to an advancing deformation process.[1–4] The previously reported results indicate that both phenomena are nearly independent of the temperature and appear to be controlled primarily by the strain applied to the material. This finding agrees with the conclusions of Hobeika et al.,[4] who demonstrated the invariance of the deformation scheme and nearly constant critical strains with respect to both the temperature and the deformation rate in polyethylene deformed in tension.

Figure 6 present an exemplary dependence of the recovered strain component [Fig. 6(a)] and the stable part, which remained after recovery at a high temperature close to the melting point of the respective polymer [Fig. 6(b)], on the strain applied. The temperatures of annealing to induce recovery were set to 125°C for linear homopolymers (melting temperature = 132–134°C), 100–110°C for branched samples L-1-L-5, LL-1, and LL-2 (melting temperature = 110–120°C), and 90°C for elastomer E-1 (melting temperature = 96°C). These temperatures were only a few degrees lower than the respective melting points of the

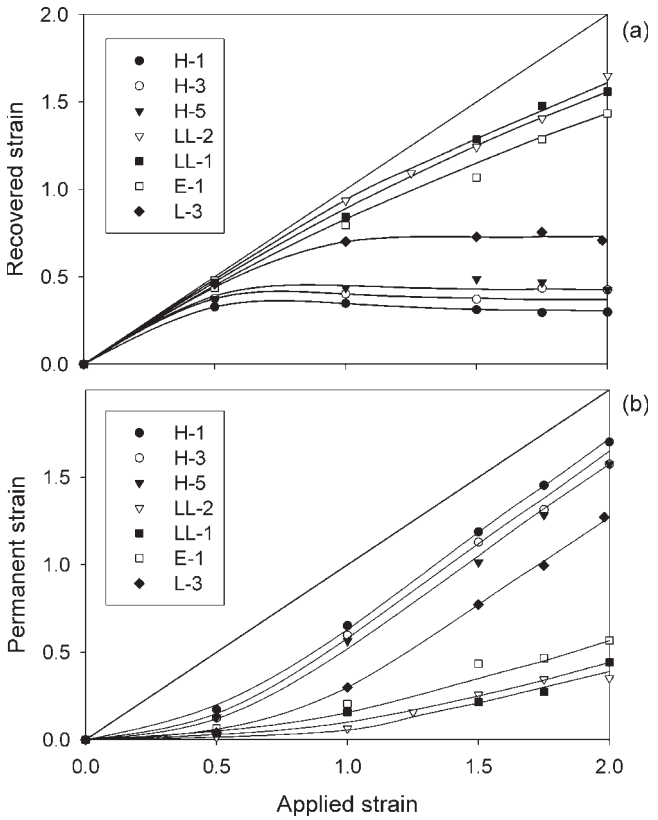

Figure 6 (a) Recovered and (b) remaining (permanent) components of the strain after recovery at a temperature near the melting point of the indicated samples (annealing temperature: 125°C for the linear homopolymers, 110°C for the L and LL samples, and 90°C for the E-1 elastomer).

crystalline phase. Therefore, the strain remaining after such annealing is probably very close to the permanent plastic strain, which would remain even after melting of the crystalline component. Unfortunately, annealing at temperatures closer to the melting point resulted in partial melting of the specimens, leading frequently to their distortion, which made the evaluation of the strain components very difficult.

Comparing the high-temperature recovery curves determined in this study (Fig. 6) with the respective curves obtained for samples deformed at room temperature,[2] we can find again a very good agreement of both sets of curves. The amount of recovered strain of the samples deformed at two notably different temperatures is very close for a given polymer and the applied compressive strain, especially for true strains below 0.6 and above 1.0. However, the deflection point of the curve of the permanent strain versus the applied strain [cf. Fig. 6(b)], which was clearly seen around the true strain of 1.0 in samples recovered after deformation at room temperature, now, for a higher deformation temperature of 80°C, shifted toward a lower strain, approximately 0.8–0.9. The transition evidenced by this characteristic change of the recovery behavior was identified previously as an onset of intense chain disentanglements[1,2,3–8] and resultant modification of the properties of the network formed by entangled chains in an amorphous component (point D of Strobl et al.'s[3] deformation scheme). Above this point, the calculated model stress–strain curves (for deformation at 80°C and at room temperature, as reported in ref. 1) departed slowly from the experimental ones, and this can be interpreted as another mark of an erosion of the network. The temperature shift of this characteristic strain can be understood easily: an increase in the deformation temperature induces an increase in the chain mobility; thus, the slippage of chains out of entanglements becomes easier, and the disentanglement process can set in earlier, at lower strain and stress levels, than deformation at room temperature. A similar small decrease in the strain at which chains become disentangled with increasing temperature of the deformation was also found in a tensile deformation mode by Hobeika et al.[4]

CONCLUSIONS

High-strain deformation in plane-strain compression at 80°C and the recovery behavior of a series of polyethylenes were studied, with special attention given to the positions of several characteristic critical strains of the deformation scheme proposed recently by Strobl et al.,[3] especially those related to the deformation of the amorphous phase: the exhaustion and locking of the interlamellar shear, triggering fragmentation of lamellae (point C), and the onset of erosion of the molecular network through chain disentanglements (D). We tried to confirm the earlier postulated invariance of that deformation scheme with respect to the temperature of deformation.[3–8] The position of point C, found around a strain of 0.6, appeared, in fact, to be practically invariant with respect to the deformation temperature. On the other hand, the critical strain at which the molecular network starts to disintegrate (point D) exhibits a weak negative temperature dependence. It shifts from a strain of 1.0 (deformation at room temperature) to a strain of 0.8–0.9 (80°C) because of increasing network relaxation. The earlier start of the chain disentanglement at a higher deformation temperature leads to a noticeable modification of the strain hardening, resulting in a decrease in the strain-hardening rate with increasing temperature. That modification depends on the molecular weight of the polymer and the architecture of the chain: the relaxation of the molecular network in low-molecular-weight samples is more intense at high temperatures than in polymers of high molecular weights. Consequently, low-molecular-weight polyethylenes show stronger reduction of the strain hard-

ening than high-molecular-weight samples, and this demonstrates strain hardening at high temperatures nearly as intense as that at room temperature, only postponed to slightly higher strains.

References

1. Bartczak, Z.; Kozanecki, M. Polymer 2005, 46, 8210.
2. Bartczak, Z. Polymer 2005, 46, 10339.
3. Hiss, R.; Hobeika, S.; Lynn, C.; Strobl, G. Macromolecules 1999, 32, 4390.
4. Hobeika, S.; Men, Y.; Strobl, G. Macromolecules 2000, 33, 1827.
5. Fu, Q.; Men, Y.; Strobl, G. Polymer 2003, 44, 1927.
6. Fu, Q.; Men, Y.; Strobl, G. Polymer 2003, 44, 1941.
7. Men, Y.; Strobl, G. J Macromol Sci Phys 2001, 40, 775.
8. Al-Hussein, M.; Strobl, G. Macromolecules 2002, 35, 8515.
9. Wunderlich, B.; Czornyj, G. Macromolecules 1977, 10, 906.
10. Haward, R. N.; Thackray, G. Proc R Soc London Ser A 1967, 302, 453.
11. Haward, R. N. Macromolecules 1993, 26, 5860.
12. Lee, B. J.; Argon, A. S.; Parks, D. M.; Ahzi, A.; Bartczak, Z. Polymer 1993, 34, 3555.
13. Galeski, A.; Bartczak, Z.; Argon, A. S.; Cohen, R. E. Macromolecules 1992, 25, 5705.
14. Haward, R. N. Polymer 1999, 40, 5821.
15. Arruda, E. M.; Boyce, M. C. J Mech Phys Solids 1993, 41, 389.
16. Boyce, M. C.; Haward, R. N. In The Physics of Glassy Polymers, 2nd ed.; Haward, R. N.; Young, R. J., Eds.; Chapman & Hall: London, 1997; p 213.
17. Arruda, E. M. Ph.D. Thesis, Massachusetts Institute of Technology, 1992.
18. Tervoort, T. A. Ph.D. Thesis, Eindhoven University of Technology, 1996.
19. Van Melick, H. G. H.; Govaert, L. E., Meijer, H. E. H. Polymer 2003, 44, 2493.
20. Treloar, L. R. G. The Physics of Rubber Elasticity, 3rd ed.; Clarendon: Oxford, 1975.
21. Smith, P.; Lemstra, P. J.; Booij, H. C. J Polym Sci Part B: Polym Phys 1981, 19, 877.
22. Smith, P.; Lemstra, P. J. Colloid Polym Sci 1980, 258, 891.
23. Bartczak, Z.; Argon, A. S.; Cohen, R. E. Macromolecules 1992, 25, 5036.